Evaluating reaction stoichiometry in magmatic systems evolving under generalized thermodynamic constraints: Examples comparing isothermal and isenthalpic assimilation

Mark S. Ghiorso and Peter B. Kelemen

Department of Geological Sciences, University of Washington, Seattle, WA 98195, U.S.A.

Abstract—Legendre transforms are utilized to construct thermodynamic potentials which are minimal in systems at thermodynamic equilibrium under conditions of fixed enthalpy, volume and chemical potential of oxygen. Numerical methods that facilitate the minimization of these potentials are described. These methods form the core of an algorithm for the calculation of reaction stoichiometry for irreversible processes in open magmatic systems proceeding under isenthalpic or isochoric constraints, or both.

As an example of the use of these methods, calculations of isothermal and isenthalpic assimilation in fractionating basaltic magma are presented. Isenthalpic calculations are most useful in considering the effects of solid–liquid reactions which are endothermic. In general, such reactions involve the assimilation of a less refractory phase in a high temperature magma, or assimilation of phases across a cotectic "valley" in the liquidus surface. The mass of crystals calculated to form during isenthalpic assimilation of pelitic rock in a magnesian MORB is six to ten times as great if the rock is assumed to be at 500°C than if the rock is at 1250°C. The examples illustrate the necessity of characterizing the temperature and phase assemblage, as well as the bulk composition, of the assimilate when considering the effect of solid–liquid reaction on the liquid line of descent.

INTRODUCTION

Chemical mass transfer in magmatic systems has been simulated previously as a succession of steps in temperature, pressure or bulk composition, with each step characterized by heterogeneous equilibrium (Ghiorso, 1985; Ghiorso and Carmichael, 1985). This approach has made possible the numerical simulation of magmatic processes such as equilibrium crystallization and crystal fractionation. This method has also proven useful in the investigation of the assimilation of solid phases (Ghiorso and Carmichael, 1985; Kelemen and Ghiorso, 1986). However, existing computational techniques are inadequate for calculation of reaction stoichiometry in thermodynamic systems evolving toward an equilibrium state under general system constraints. By general constraints we mean those other than temperature (T), pressure (P) and fixed bulk composition. There are two reasons for this inadequacy. Firstly, the Gibbs free energy, G, is not necessarily minimal in a thermodynamic system that is generally constrained. Thus, to calculate heterogeneous equilibrium at each step in a mass transfer calculation, proceeding under a specified set of generalized constraints, requires the generation of a thermodynamic potential which is minimal under these conditions. The second difficulty is computational. Constraints other than temperature, pressure or fixed bulk composition are usually non-linear functions of their independent variables, *i.e.,* the enthalpy, H, is a non-linear function of temperature, pressure and the number of moles of system components. Therefore, after deduction of the appropriate potential, its minimum must be computed by finding those particular values of the independent variables of the system that satisfy the non-linear constraint(s). This is a formidable numerical problem, which in magmatic systems has only been attempted in an approximate fashion (Ghiorso, 1985).

In this paper we review the theory behind the construction of potentials which are minimal in systems subject to generalized thermodynamic constraints. This theory is rendered practical for computational purposes by a modification of the numerical algorithm utilized by Ghiorso (1985) along the lines suggested by Gill *et al.* (1981). These general procedures are applied to evaluate reaction stoichiometry in magmatic systems evolving under isenthalpic or isochoric constraints, or both. In addition, a more rigorous treatment of the calculation of equilibria in thermodynamic systems open to a perfectly mobile component (Korzhinskii, 1959; Thompson, 1970) is given. Numerical examples that model assimilation in magmas under both isothermal and isenthalpic conditions are provided. These examples illustrate the utility of the technique in predicting the effects of assimilation on derivative liquids.

CONSTRUCTION OF THERMODYNAMIC POTENTIALS

In this section we utilize mathematical methods for defining thermodynamic potentials which have been described by CALLEN (1961) and THOMPSON (1970). Let Ψ be an unspecified thermodynamic potential which is minimal at equilibrium. This minimum is constrained by the specification of linear and possibly non–linear relationships among the independent variables of Ψ. For example, if $\Psi = G(T, P, n_1, n_2, \ldots, n_c)$, where n_1, n_2 to n_c are variables denoting the number of moles of each of the c system components in each phase, then G is minimal at equilibrium subject to constant temperature, pressure and fixed *bulk* composition. The latter constraint does not imply that n_1 through n_c must be held constant in the processes of minimizing G, but rather that *linear* combinations of the n_1 through n_c must be constrained in order that the system bulk composition remain constant. There will always be more n_i's than compositional variables in a *multi*–phase thermodynamic system. Mathematically, finding the minimum of G is simply a case of optimizing a non–linear function subject to linear equality constraints.

Let the independent variables of Ψ be denoted by x, y, n_1, n_2, \ldots, n_c. For convenience, we will group the mol numbers of the various system components to form the elements of a vector denoted by n such that:

$$n = \begin{bmatrix} n_1 \\ n_2 \\ \cdot \\ \cdot \\ \cdot \\ n_c \end{bmatrix}. \tag{1}$$

Thus, we may write $\Psi = \Psi(x, y, n)$. If a new thermodynamic potential, Φ, is to be defined such that $\Phi = \Phi((\partial \Psi/\partial x)_{y,n}, y, n)$, then Φ is given by the Legendre transform (CALLEN, 1961) of Ψ:

$$\Phi\left(\left(\frac{\partial \Psi}{\partial x}\right)_{y,n}, y, n\right) = \Psi(x, y, n) - x\left(\frac{\partial \Psi}{\partial x}\right)_{y,n}. \tag{2}$$

As an example, we might consider the case treated by THOMPSON (1970) and GHIORSO (1985) of a perfectly mobile component. Imagine a magmatic system whose boundaries are open to oxygen exchange such that the chemical potential of oxygen in the system is fixed by external constraints. By denoting this chemical potential μ_{O_2}, we seek a new potential, Φ, which is minimal at equilibrium in this partially open magmatic system at constant temperature and pressure. By recognizing that μ_{O_2} is defined as $(\partial G/\partial n_{O_2})_{T,P,n^*}$, where n^* denotes all mole numbers held constant except those of oxygen, the potential Φ can be expressed as [Equation (2)]:

$$\Phi = G - n_{O_2}\mu_{O_2}. \tag{3}$$

Potentials of the form of Equation (3), which are minimal in systems open to perfectly mobile components, are usually referred to as Korzhinskii potentials (THOMPSON, 1970).

We now utilize Equation (2) to construct a number of thermodynamic potentials which are useful in calculating reaction paths in magmatic systems.

Isenthalpic constraints

We seek the potential $\Phi(H, P, n_1, n_2, \ldots, n_c)$. From the definition of the Gibbs free energy a new potential may be defined:

$$G/T = H/T - S. \tag{4}$$

The total derivative of G/T may be deduced from Equation (4):

$$d\left(\frac{G}{T}\right) = Hd\left(\frac{1}{T}\right) + \frac{1}{T}dH - dS,$$

and given that

$$dH = TdS + VdP + \sum_{i=1}^{c} \mu_i dn_i,$$

we have:

$$d\left(\frac{G}{T}\right) = Hd\left(\frac{1}{T}\right) + \left(\frac{V}{T}\right)dP + \left(\frac{1}{T}\right)\sum_{i=1}^{c} \mu_i dn_i. \tag{5}$$

Equation (5) demonstrates that

$$\left(\frac{\partial G/T}{\partial 1/T}\right)_{P,n} = H,$$

which allows us to write, by using Equation (2):

$$\Phi(H, P, n) = \frac{G}{T} - \frac{1}{T}\left(\frac{\partial G/T}{\partial 1/T}\right)_{P,n}$$

$$= \frac{G}{T} - \frac{1}{T}H$$

$$\Phi(H, P, n) = -S. \tag{6}$$

Equation (6) establishes that equilibrium in a closed system subject to constant enthalpy and pressure is given by a maximum in entropy.

Isochoric constraints

In this case we seek the function $\Phi(T, V, n)$. The formalism of the Legendre transform is unnecessary

in the case of isochoric constraints as the required function Φ is just the Helmholtz free energy, denoted by the symbol A:

$$\Phi(T, V, n) = A = G - PV. \qquad (7)$$

Combined isenthalpic and isochoric constraints

Under conditions of constant enthalpy and volume the potential Φ can be obtained from Equation (5) by recognizing that

$$\left(\frac{\partial G/T}{\partial P}\right)_{(1/T),n} = \frac{V}{T},$$

from which the Legendre transform may be constructed as:

$$\Phi(H, V, n) = \frac{G}{T} - \frac{1}{T}\left(\frac{\partial G/T}{\partial 1/T}\right)_{P,n} - P\left(\frac{\partial G/T}{\partial P}\right)_{(1/T),n}$$

$$= \frac{G}{T} - \frac{1}{T}H - P\frac{V}{T}$$

$$\Phi(H, V, n) = -S - \frac{VP}{T}. \qquad (8)$$

Equation (8) establishes the potential which is minimal under conditions of constant enthalpy, volume and fixed bulk composition.

THE MATHEMATICAL PROBLEM OF MINIMIZING Φ

In order to calculate heterogeneous equilibrium with the chemical mass transfer algorithm of GHIORSO (1985) we require a numerical method to minimize the newly defined functions, Φ, subject to the appropriate constraints. To formulate correctly the problem we must recognize initially that the fixed bulk composition constraints are always linear functions of the system components. From GHIORSO (1985) we define the rectangular matrix C such that

$$Cn = b, \qquad (9)$$

where b is a vector which describes the bulk composition of the system in terms of a minimal set of linearly independent compositional variables. As mentioned above, the length of n is greater than or equal to the length of b. Equation (9) embodies linear constraints in that the matrix C is not a function of n.

The optimization of Φ with respect to n (and possibly T and P) can be written with the aid of Equation (9) as:

minimize $\Phi(x, y, n)$

such that

$$Cn - b = 0$$

$$\Delta x(n, T, P) = 0$$

and

$$\Delta y(n, T, P) = 0. \qquad (10)$$

From examination of Equation (10) it is clear that the calculation of heterogeneous equilibrium in generally constrained thermodynamic systems is essentially a problem in non–linear optimization subject to *non*–linear constraints. A numerical method for the solution of Equation (10) is provided in Appendix A.

THE ADDITION OF PERFECTLY MOBILE COMPONENTS

The necessity of modelling phase equilibria in magmatic systems open to oxygen exchange has been discussed by GHIORSO (1985), GHIORSO and CARMICHAEL (19850 and CARMICHAEL and GHIORSO (1986). This need arises out of a lack of knowledge regarding relevant oxidation–reduction couples which buffer the ferric/ferrous ratio in a crystallizing magma. For modelling purposes it is convenient to approximate the effect of these unknown homogeneous redox equilibria by specifying the chemical potential of oxygen in the system. GHIORSO (1985) formulated a solution to the minimization of the Korzhinskii potential for open system oxygen exchange by approximating the non–linear equality constraint corresponding to fixed chemical potential of oxygen in the system with an empirical linearized constraint. This formulation is adequate for many calculations, but is not an exact solution to the problem. With the algorithm discussed in Appendix A, it is possible to formulate the problem exactly.

A comprehensive expression for the chemical potential of oxygen in a magmatic liquid is provided by KILINC *et al.* (1983). Its value is a function of the fugacity of oxygen, temperature, pressure, the ferric/ferrous ratio in the melt and the number of moles of various liquid components. The Korzhinskii potential, which is minimized under equilibrium conditions in this open system, is given by (see above):

$$\Phi = G - n_{O_2}\mu_{O_2}. \qquad (11)$$

We take n_{O_2} to be the number of moles of oxygen produced or consumed in the course of crystallization; indexed by the relative increase or decrease in the ferric/ferrous ratio of the system necessary to maintain constant μ_{O_2}. The minimum in Φ is

calculated subject to fixed T, P, μ_{O_2} and bulk composition with the provision of variable ferric/ferrous ratio. The optimal variables are the system components, n. Numerical methods suitable for minimizing the open system potential defined by Equation (11) are discussed in Appendix A. In Appendix B appropriate matrices and vectors needed for the minimization algorithm are derived and the results generalized to the case of the calculation of heterogeneous equilibrium in chemical systems open to oxygen and subject to isenthalpic and/or isochoric constraints.

AN ALGORITHM FOR CHEMICAL MASS TRANSFER IN MAGMATIC SYSTEMS SUBJECT TO GENERALIZED CONSTRAINTS

After having established the means of calculating heterogeneous equilibrium in arbitrarily constrained, open magmatic systems, we can now summarize a method for the calculation of chemical mass transfer in such systems. In isothermal, isobaric open magmatic systems, the appropriate Korzhinskii potential is minimized at each step in reaction progress. This calculational scheme is identical to the free energy minimization method described by GHIORSO (1985). In systems subject to isochoric or isenthalpic constraints, the initial step in calculating the evolution of the system involves determining the heterogeneous phase assemblage by minimization of the Gibbs free energy or relevant Korzhinskii potential for the system. This establishes an initial "equilibrium" volume or enthalpy which can then be used to constrain the equilibrium "path" of all future steps in reaction progress. A typical calculation might involve determining the stable solid–liquid assemblage for a magma at a given temperature and pressure, and modelling isenthalpic assimilation by adding small increments of solid to the magma, keeping track of the attendant changes in system bulk composition and increase in total system enthalpy due to the added enthalpy of the solid. At each incremental step of solid addition a new equilibrium solid–liquid phase assemblage and temperature are calculated at the new system bulk composition and total enthalpy. By choosing small enough steps, the continuous irreversible process of isenthalpic assimilation can be modelled. By examination of the compositions and proportions of solid and liquid produced at each increment of reaction progress, the stoichiometry of the assimilation reaction can be determined.

Software has been designed to implement the non–linearly constrained optimization algorithm described in Appendix A in order to allow the modelling of isenthalpic, isochoric, isothermal and isobaric reactions in magmatic systems open to oxygen. This software constitutes version 2.0 of the program SILMIN (GHIORSO, 1985). Source code is available from the first author. Thermodynamic data essential for the numerical implementation of this algorithm are summarized by GHIORSO *et al.* (1983) and GHIORSO (1985). Some applications of these calculations in magmatic systems are presented below.

APPLICATIONS

Assimilation of wall rock into basaltic magma has been proposed to explain a range of chemical variation trends in igneous rock series. BOWEN (1922a) explained the basic principles for thermodynamic treatment of solid–liquid reaction in silicate systems. Few subsequent studies of interaction between magma and wall rock have taken this approach, probably due to the scarcity of data on the slope of the multi–component liquidus surface, heats of fusion of solid solutions, and heats of mixing in silicate liquids. Further investigation may also have been discouraged by BOWEN's assertion that assimilation processes could not produce liquids fundamentally different from those produced by fractional crystallization alone. BOWEN (1922a) showed how, in the forsterite–anorthite–silica system determined by ANDERSON (1915), assimilation of olivine in liquids could alter the crystal and liquid line of descent. However, he believed that all such phenomena were of secondary importance, because all liquids in the ternary still possess the theoretical capacity to fractionate toward the same eutectic composition. As emphasis in igneous petrology has changed from debate over the ultimate destination of liquid fractionation to explanation of the variation between different lines of descent, the potential effect of combined assimilation and crystallization has become a subject of increasing interest.

BOWEN (1922a) showed that, for the silicate systems which had been determined experimentally by 1922, heats of mixing were negligible by comparison with heats of fusion. This observation has generally been supported by recent work. Unlike the dissolution of salts in aqueous solution, which could evolve heat without consequent crystallization, the pure dissolution of silicate minerals in magma would be endothermic. Important exceptions include the heats of fusion of the silica polymorphs β–quartz, tridymite and β–cristobalite. These enthalpies are relatively small, on the order of 30 cal/gm, in the range of estimated heats of mixing in natural silicate liquids (GHIORSO and CARMICHAEL, 1980).

In developing examples in the continuous and discontinuous reaction series (defined in BOWEN, 1922b), BOWEN (1922a,b) showed that the dissolution of refractory phases in liquids in equilibrium with less refractory phases in the same series, at constant temperature, causes crystallization of the phases with which the magma is saturated. This process maintains the composition of the magma on the liquidus surface; magma composition on the liquidus in a binary system is isothermally, isobarically invariant, whereas in a ternary system the composition may be univariant or invariant. In the examples given (BOWEN, 1922a, pp. 523–537), the mass crystallized was calculated to be larger than the mass dissolved; BOWEN (1922a) suggested that such reactions would generally be exothermic.

Similarly, BOWEN (1922a) developed examples of assimilation of less refractory phases in liquids saturated with higher–temperature phases. In the examples, it was shown that the energy required to dissolve the assimilate could not normally be provided by the heat capacity of the magma, because known heats of fusion, per gram, for silicates were two or three orders of magnitude larger than liquid heat capacities, which BOWEN (1922a) estimated at 0.2 to 0.3 cal/gm °C. The result of dissolving a low-temperature melting member of the reaction series, he reasoned, is a drop in temperature, followed by crystallization of a smaller mass of the phase(s) with which the magma is saturated.

Schematic illustration of these relationships is given in Figure 1. Note that the assimilation of a refractory phase in liquid saturated in a less refractory phase in the same reaction series, at constant temperature, need not always be exothermic. Instead,

$$\Delta H = Ma\Delta H_f^a - Mc\Delta H_f^c, \qquad (12)$$

for Ma equal to the mass assimilated, Mc equal to the mass crystallized, and ΔH_f^a and ΔH_f^c equal to the apparent heats of fusion, per gram, of the assimilate and the resultant crystals, respectively. Apparent heats of fusion are the heats of fusion of the solids at some temperature, T', below the melting temperature of the pure solid. They are calculated as:

$$\Delta H_f = \Delta H_F + \int_{T'}^{T_m} C_{P,\text{solid}}\,dT - \int_{T'}^{T_m} C_{P,\text{liquid}}\,dT, \quad (13)$$

where ΔH_f is the apparent heat of fusion at T', ΔH_F is the heat of fusion of the pure substance at its melting temperature, T_m is the melting temperature of the pure substance, and $C_{P,\text{solid}}$ and $C_{P,\text{liquid}}$ are the heat capacities of pure solid and liquid over the temperature range T_m-T'. The magnitude and sign

A = FORSTERITE ΔH_f^a = 200 cal/gm
C = ENSTATITE ΔH_f^c = 155 cal/gm   at 1300°C

$\Delta T = [Mc\,\Delta H_f^c - Ma\,\Delta H_f^a] / M_{TOT}\,C_P^{TOT}$

$\Delta T = 0$ Ma/Mc = 0.78

A = DIOPSIDE ΔH_f^a = 151 cal/gm
C = FORSTERITE ΔH_f^c = 200 cal/gm   at 1300°C

ΔT cannot be > or = 0 (?)
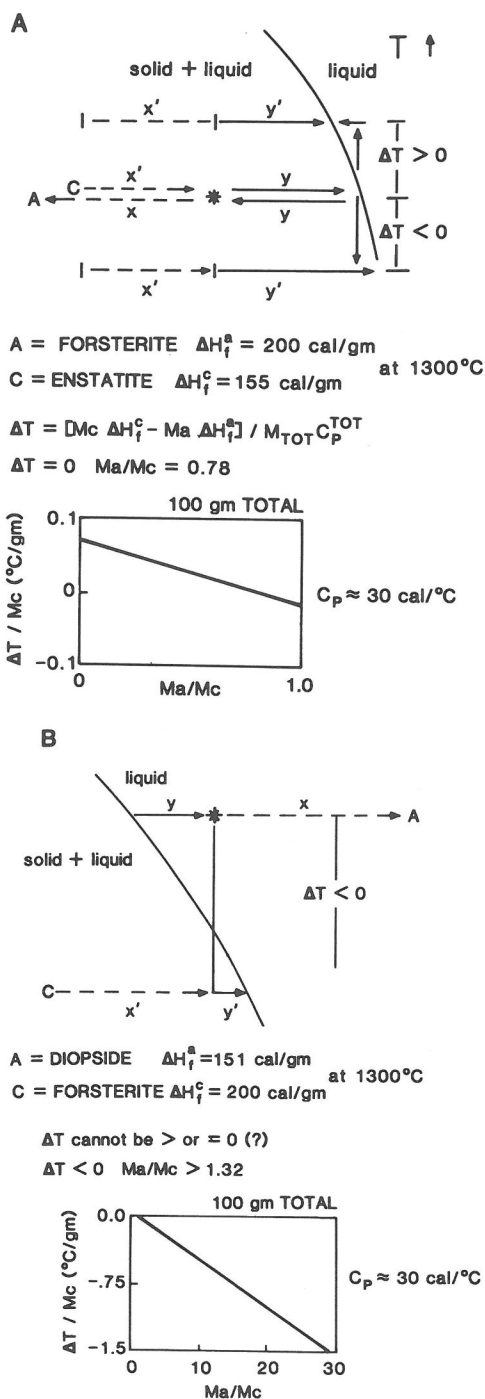
$\Delta T < 0$ Ma/Mc > 1.32

FIG. 1. (A) Schematic representation of assimilation of a refractory phase in liquid saturated with a less refractory member of the same reaction series. Resultant crystal and liquid products are shown for the cases of isothermal and isenthalpic assimilation. (B) Similar representation, for assimilation of a less refractory phase in a liquid saturated with a member of the same reaction series, or assimilation across a cotectic "valley".

of ΔH in Equation (12) may vary depending on the ratios Ma/Mc and $\Delta H_f^a/\Delta H_f^c$.

The ΔH for assimilation of a refractory phase in a magma saturated with a phase lower in the same reaction series will often be negative, but may be very close to zero. For example, take the assimilation of magnesian olivine in a liquid saturated with low-calcium pyroxene. In the Mg_2SiO_4–SiO_2 system, BOWEN (1922a,b) calculated Ma/Mc approximately equal to 0.2 at 1550°C. Assuming $\Delta H_f^{Fo} = 238$ cal/gm and $\Delta H_f^{En} = 186$ cal/gm (data on ΔH_F and liquid and solid heat capacities from ROBIE et al., 1978, STEBBINS et al., 1984, and GHIORSO and CARMICHAEL, 1980), $Ma/Mc = 0.2$ corresponds to an enthalpy change of -138 cal per gram clino–enstatite crystallized at 1550°C. In natural basaltic to andesitic liquids, KELEMEN (1986) and KELEMEN and GHIORSO (1986) calculate a range of Ma/Mc for the reaction olivine + liquid = orthopyroxene; a reasonable average might be 0.6. For this reaction stoichiometry, with $\Delta H_f^{Fo} \simeq 185$ cal/gm and $\Delta H_f^{En} \simeq 142$ cal/gm at 1200°C, the enthalpy change would be close to -31 cal per gram orthopyroxene produced.

During assimilation of a less refractory phase, or assimilation of material across a cotectic "valley", ΔH will always be positive. For instance, assimilation of diopside in liquid saturated with forsterite in the system forsterite–diopside–anorthite (OSBORN and TAIT, 1952) must be endothermic at constant temperature. The process of dissolving diopside will move the liquid off the forsterite liquidus surface. There will be no limit to the enthalpy change produced by this reaction until the liquid is saturated in diopside. Until then, ΔH will be positive, increasing by 151 cal per gram diopside dissolved (ΔH_f^{Di} at 1300°C from ROBIE et al., 1978; GHIORSO and CARMICHAEL, 1980; STEBBINS et al., 1984). If a reservoir of forsterite is initially present in the system, dissolution of diopside at constant temperature will lead to dissolution of forsterite as well. Note that these effects are qualitatively similar to the effects of assimilation of forsterite in liquid saturated with diopside.

If, instead of constant temperature, the system were constrained to constant enthalpy, then the temperature would drop, such that;

$$\Delta T = [Ma\Delta H_f^a - Mc\Delta H_f^c]/M^{tot}C_p^{tot}, \quad (14)$$

where M^{tot} is equal to the total mass of the system and C_p^{tot} is the heat capacity of the system (about 0.3 cal/gm °C, assuming the masses of the solid phases are negligible relative to the mass of liquid). For assimilation of a less refractory phase in the same reaction series, or assimilation across a cotec-

tic, ΔT must be less than zero. In the particular case of diopside dissolving in liquid saturated in forsterite at 1300°C, this requires Ma/Mc to be greater than about 1.3, and for assimilation of forsterite in diopside saturated liquid, Ma/Mc must be greater than 0.75.

The foregoing discussion applies to dissolution and consequent crystallization where the assimilate is at magmatic temperature prior to reaction. Where this is not the case, the energy required to heat the assimilate to magmatic temperature must also be included in the calculation of mass and energy balance at constant temperature or constant enthalpy. Again, BOWEN (1922a) treated this problem. He noted that the heat of crystallization of saturated phases can supply the energy needed to heat inclusions or wall rock, or both. Because heats of fusion are orders of magnitude greater than heat capacities in silicate systems, per gram, crystallization of a mass of liquid can raise the temperature of an equal mass of solids tens, or even hundreds, of degrees.

All these relations apply in principle to reactions in natural systems. However, in practice, such calculations have been limited by lack of quantitative understanding of such important variables as the slope of the liquidus surface in pressure-temperature-composition space. Development of a solution model for silicate liquids (GHIORSO et al., 1983; GHIORSO, 1985; GHIORSO and CARMICHAEL, 1985), implemented in the computer program SILMIN, permits investigation of solid–liquid reaction stoichiometry in natural systems (e.g., GHIORSO, 1985; KELEMEN, 1986; KELEMEN and GHIORSO, 1986).

Constant temperature may be an unreasonable constraint for assimilation of low melting phases, or assimilation of phases across a cotectic. During such exothermic reactions, magmatic temperature cannot often be externally buffered at a constant value. It is easier to understand and apply the results of calculations constrained to constant enthalpy. Isenthalpic calculations may provide a close approach to some important natural phenomena.

To illustrate the relevance of such calculations, we present the following example. In Figure 2, we have shown liquid compositions in the system forsterite–diopside–anorthite (OSBORN and TAIT, 1952), which are saturated in forsterite, and will fractionate to the forsterite–diopside cotectic. Isothermal assimilation of anorthite, on the other hand, moves the magma composition off the liquidus towards the anorthite apex, first dissolving any reservoir of forsterite in the system, until it is saturated in anorthite. Schematic, isenthalpic assimilation paths are depicted as well; given a knowledge of the

heats of fusion of anorthite and forsterite, and the heat capacity of the system, combined with the lever rule, such approximate paths are simple to determine. The liquid in the isenthalpic assimilation case fractionates to the anorthite field (case 1), or to the forsterite–anorthite cotectic (case 2), with decreasing temperature. At points C1 and C2 (Figure 2), the liquid will not dissolve further anorthite added to the system; its composition and temperature will remain constant.

Figure 3 and Table 1 illustrate some of the results of a similar calculation, by using a natural system: a magnesian MORB, FAMOUS 527-1-1 (BENDER *et al.,* 1978) plus 2 weight percent H_2O at 1 kbar, constrained to react along the FMQ oxygen buffer. This wet basalt is calculated to crystallize olivine, beginning at about 1223°C, followed by clinopyroxene at about 1165°C, and plagioclase (An_{77}) at about 1095°C. Isenthalpic assimilation of anorthite ($T_{solid} = 1225°C$) in this basalt, beginning at 1225°C, leads to a decrease in temperature, accompanied by crystallization of olivine beginning at about 1208°C, and plagioclase (An_{87}) at 1162°C. The calculated temperature then rises, as continued assimilation of anorthite results in the precipitation of a larger mass of increasingly calcic plagioclase. The total mass of solids produced in the temperature interval 1225 to 1165°C is much greater in the equilibrium crystallization calculation than in the case of isenthalpic assimilation of anorthite.

In order to test the notion that isenthalpic assimilation of more refractory phases in crystallizing magma might be similar in its effect to isothermal assimilation, we compared the two paths for assimilation of magnesian olivine in FAMOUS 527-1-1, dry, at 3 kbar, evolving along the FMQ oxygen

FIG. 3. Calculated total solid composition for equilibrium crystallization and isenthalpic assimilation of anorthite in a magnesian MORB (FAMOUS 527-1-1 + 2 weight percent H_2O) at 1 kbar, on the FMQ oxygen buffer. This, and all subsequent calculations depicted in Figures 4 through 7, were performed using the computer program SILMIN, described in the text. Input parameters are the initial composition of the system, temperature, pressure, oxygen fugacity, and the composition and temperature of the assimilate. Resultant liquid and solid compositions, phase proportions, and temperatures in the isenthalpic case, are calculated. Initial temperature of the liquid, and the temperature of the assimilate throughout the calculation, was set at 1225°C.
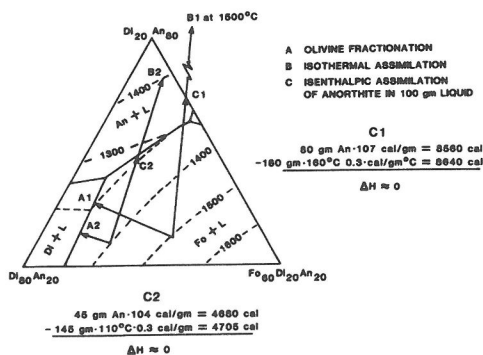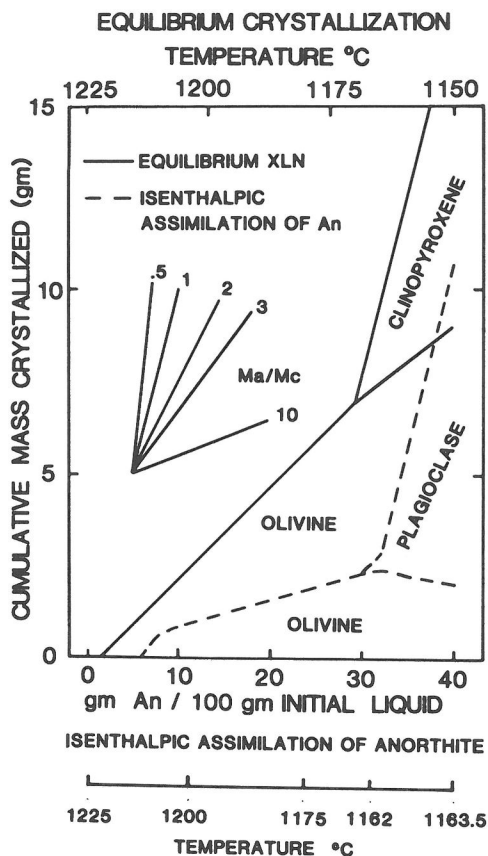

FIG. 2. (A) Paths for crystal fractionation, (B) isothermal assimilation of anorthite, (C) and isenthalpic assimilation of anorthite, for liquids (1 and 2) saturated with forsterite in the forsterite–diopside–anorthite system, determined by OSBORN and TAIT (1952).

buffer. Results are summarized in Figure 4 and Table 2. Resultant crystal and liquid compositions are almost identical in the isothermal and isenthalpic cases. In both cases, dissolution of olivine (Fo_{90}) leads to crystallization of a slightly larger mass of more iron–rich olivine, accompanied by a small percentage of plagioclase in the isothermal case. In the isenthalpic case, the calculated temperature rises 3°C during assimilation of 40 grams of Fo_{90}. Despite the rather simple reaction stoichiometry ($Fo_{90} + liq = Fo_{87}$, with *Ma/Mc* of about 0.9), this reaction

M. S. Ghiorso and P. B. Kelemen

Table 1. Calculated total solid composition produced during the assimilation of anorthite in FAMOUS 527-1-1 + 2 weight percent H_2O, 1 kbar, on the FMQ oxygen buffer.

	Initial	Isothermal	Isenthalpic
Mass Assimilated/100 gm initial liquid + crystals	0	40	40
Initial Temperature of Anorthite	—	1225°C	1225°C
Total Mass Crystallized (gm)	0	0	10.72
Mass Olivine (gm) Mol Fraction Fo	0*	0	2.11 0.82
Mass Plagioclase Mol Fraction An	0	0	8.61 0.88
Temperature of the System	1225°C	1225°C	1164°C†

* 0.27 gm Fo_{82} @ 1220°C.

† Minimum temperature @ 1162°C, 32 gm assimilated with 2.36 gm Fo_{82} and 0.43 gm An_{87} crystallized.

has an important effect on the liquid line of descent, because the conversion of Fo_{90} to Fo_{87} fractionates FeO from the magma, effectively buffering the magnesium number (Mg#) of the derivative liquid. Similar reactions between high temperature wall rock and fractionating basalt in the upper mantle are likely. Their effects are more fully discussed by KELEMEN (1986).

ISENTHALPIC ASSIMILATION OF OLIVINE (1250°C)

FIG. 4. Calculated total solid composition for isothermal and isenthalpic assimilation of olivine (Fo_{90}) in a magnesian MORB (FAMOUS 527-1-1), dry, at 3 kbar, on the FMQ oxygen buffer. Initial temperature of the liquid, and the temperature of the assimilate throughout the calculation, was set at 1250°C. *Ma/Mc* refers to the ratio of mass assimilated vs. mass crystallized.

Initial temperature of the assimilate is the most important variable in considering the potential effects of assimilation of wall rock by magmas in the crust. Although the notion of assimilation of low melting pelitic or quartzo–feldspathic metasediments, or both, in high temperature, basaltic melts has an immediate, intuitive appeal, this process is strongly endothermic and cannot be viewed simply as bulk melting and mixing of a crustal component. To illustrate this point, already made on semi–quantitative grounds by BOWEN (1922a), we have made calculations modelling the assimilation of pure albite, and a composite pelitic composition, in a magnesian MORB.

The initial liquid composition used was FAMOUS 527-1-1, dry, at 3 kbar, constrained to react along the FMQ oxygen buffer, at an initial temperature of 1250°C. We first compare the predicted equilibrium crystallization path for this liquid to the experimental results of BENDER *et al.* (1978) on this composition. Results of calculations using SILMIN have olivine (Fo_{87}) on the liquidus at 1290°C, followed by plagioclase (An_{82}) at 1245°C, and clinopyroxene (Di_{85}) at 1235°C. Comparable values from the experiments at 1 bar are olivine ($Fo_{89.5}$) at 1268°C, and plagioclase (An_{89}) at 1235°C. At 6 kbar, oliving (Fo_{87}) appears at 1280°C, followed by plagioclase (An_{78}) at 1240°C. Clinopyroxene first crystallized between 1135 and 1150°C, at 1 bar, and between 1240 and 1250°C, at 6 kbar. Low–calcium pyroxene was not observed in any experimental runs.

Three different reaction paths were modelled: (1) isothermal assimilation, with the solid assimilate at 1250°C (a metastable solid state, at least in the case of albite); (2) isenthalpic assimilation, with the assimilate at 1250°C; and (3) isenthalpic assimilation
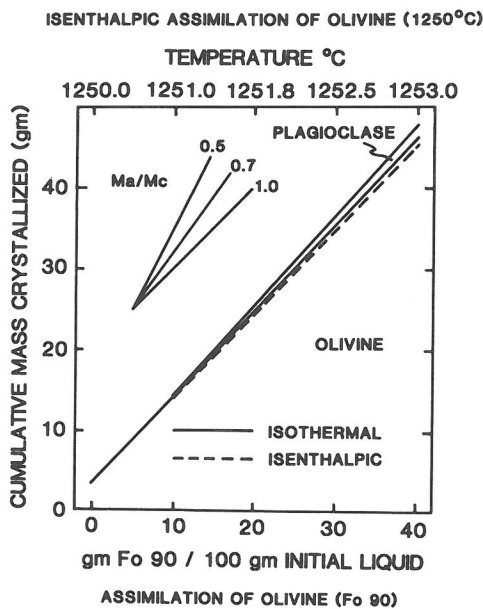
Table 2. Calculated total solid composition produced during the assimilation of olivine (Fo$_{90}$) in FAMOUS 527-1-1, at 3 kbar, on the FMQ oxygen buffer.

	Initial	Isothermal	Isenthalpic
Mass Assimilated/100 gm initial liquid + crystals	0	40	40
Initial Temperature of Olivine	1250°C	1250°C	1250°C
Total Mass Crystallized (gm)	3.44	50.55	46.44
Mass Olivine (gm)	3.44	47.71	46.44
Mol Fraction Fo	0.867	0.863	0.866
Mass Plagioclase	0	2.84	0
Mol Fraction An		0.823	
Temperature of the System	1250°C	1250°C	1253.5°C

with the assimilate at 500°C. In modelling assimilation of pelitic rock, we used a bulk composition derived by averaging the group analyses for shale and slate reported by CLARKE (1924). This composition was recast as proportions of two mineral assemblages: assemblage A (quartz–K feldspar–ilmenite–orthopyroxene–spinel–plagioclase), representative of pelitic rocks in granulite and pyroxene hornfels facies; and assemblage B (quartz–muscovite–ilmenite–biotite–garnet–plagioclase), representative of pelitic rocks in amphibolite facies. Thermodynamic data for most of these solid phases are summarized by GHIORSO et al. (1983) and constitutes part of the SILMIN data base. Data for

muscovite, phlogopite, annite, pyrope, and almandine are from HELGESON et al. (1978). Note that the phase assemblages are somewhat arbitrary. For instance, under most conditions, spinel + quartz break down to orthopyroxene + alumino–silicate. However, by use of spinel rather than sillimanite was more convenient for computational reasons. Similarly, all iron has been arbitrarily assumed to be ferrous iron. The bulk composition used and the proportions of mineral end–members are given in Table 3.

Some of the results of modelling assimilation of albite and pelitic rock are given in Figures 5, 6, and 7 and Tables 4 and 5. Figures 5 and 6 summarize

Table 3. Pelitic composition used in assimilation calculations. This composition was derived by averaging the group analyses for shale and slate reported by CLARKE (1924, pp. 552 and 631) H$_2$O, CO$_2$, SO$_2$, C, P$_2$O$_5$ and trace components in the analyses were ignored; other oxides normalized to 100 weight percent.

Bulk composition		Phase assemblage A		
	Weight percent		Mol percent	Weight percent
SiO$_2$	64.463	Hercynite	Hc$_{58}$	4.94
		Spinel	Sp$_{42}$	2.93
TiO$_2$	0.731	Enstatite	En$_{46}$	4.80
		Ferrosilite	Fs$_{54}$	7.33
Al$_2$O$_3$	17.107	Sanidine		21.02
		Albite	Ab$_{48}$	13.48
FeO*	6.691	Anorthite	An$_{52}$	15.40
		β–Quartz		28.72
MgO	2.754	Ilmenite		1.39
CaO	3.105	Phase assemblage B		
Na$_2$O	1.593	Almandine	Alm$_{61}$	3.66
		Pyrope	Py$_{39}$	1.92
K$_2$O	3.556	Phlogopite	Phl$_{47}$	7.20
		Annite	Ann$_{53}$	10.19
Phase assemblage B also includes		Muscovite		14.01
1.35 weight percent H$_2$O in		Albite	Ab$_{48}$	13.48
biotite and muscovite.		Anorthite	An$_{52}$	15.40
		α–Quartz		32.75
		Ilmenite		1.39

ISENTHALPIC ASSIMILATION OF ALBITE (1250°C)

TEMPERATURE °C

1250.0 1237.7 1227.5 1218.9 1211.8

ASSIMILATION OF ALBITE (1250°C)

TEMPERATURE °C

1250 1223 1203 1187 1170
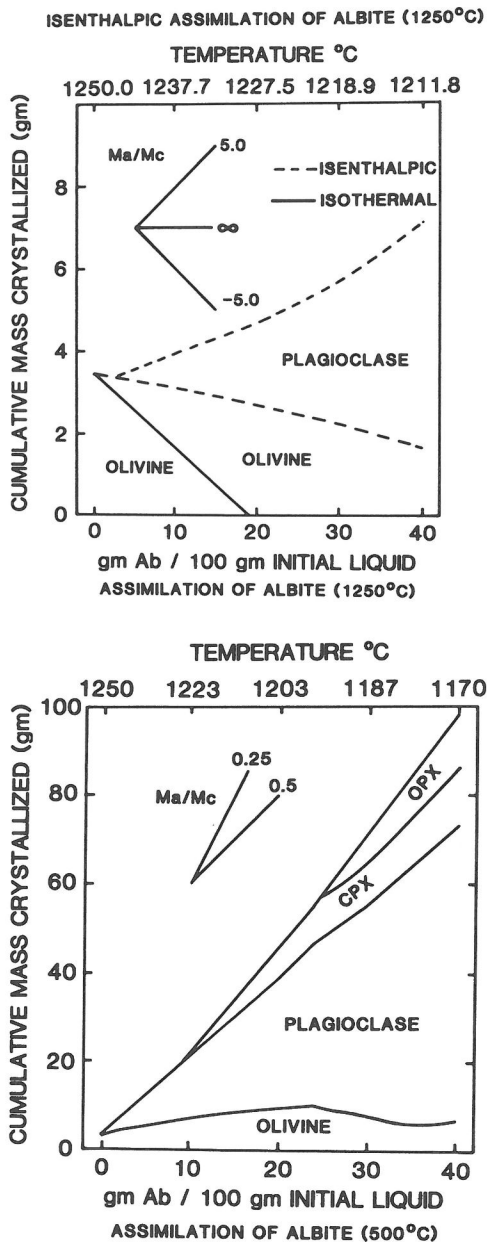
ASSIMILATION OF ALBITE (500°C)

FIG. 5. (A) Calculated total solid composition for iso-thermal and isenthalpic assimilation of albite in a mag-nesian MORB (FAMOUS 527-1-1), dry, at 3 kbar, on the FMQ oxygen buffer. Initial temperature of the liquid, and the temperature of the assimilate throughout the calcu-lation, was set at 1250°C. *Ma/Mc* refers to the ratio of mass assimilated vs. mass crystallized. (B) Input parameters as in 5(A), but with the temperature of the assimilate set at 500°C throughout the calculation.

calculated solid compositions. Note that the vertical scale (cumulative mass crystallized) is ten times as large for reaction with the assimilate at 500°C than

for reaction with the assimilate at 1250°C. Whereas isenthalpic assimilation of 40 grams of albite and pelitic rock at 1250°C have been calculated to pro-duce less than 10 grams of olivine and plagioclase, isenthalpic dissolution of the same two phase as-semblages at 500°C is predicted to result in crys-tallization of almost 100 grams of plagioclase and pyroxene. This difference results entirely from the energy requirements of heating the assimilate to magmatic temperatures. Dissolution of the high temperature solids leads to a decrease of 35 to 40°C in the temperature of the system. Dissolution of the 500°C solids leads to a decrease of 70 to 80°C.

It is also important to consider the differences between assimilation of pelitic phase assemblages A and B, both at 500°C. Phase assemblage A might be thought of as a granulite facies rock which cooled to 500°C after the peak of metamorphism. Phase assemblage B, characteristic of pelitic rocks in am-phibolite facies, includes muscovite and biotite. Equilibrium dissolution of these hydrous minerals in fluid undersaturated magma saturated with ol-ivine, pyroxenes, and plagioclase, can be thought of as a combination of three discrete steps: (1) de-hydration reactions (such as biotite + 3 muscovite = 4 Kspar + 3 spinel + 4 H_2O); (2) melting of the dehydrated solid phases; and (3) solution of the new melt, plus H_2O, in the assimilating magma. Because dehydration reactions, like melting reactions, are endothermic at crustal pressures, the apparent en-thalpy of fusion of a hydrous assemblage will gen-erally be larger than the apparent enthalpy of fusion of an equivalent anhydrous assemblage.

We reasoned that isenthalpic assimilation of a phase assemblage including muscovite and biotite would result in a larger temperature drop, per gram assimilated, and thus (at the same bulk composi-tion) more crystallization from the derivative liquid, compared to assimilation of an assemblage with Kspar and spinel replacing the hydrous phases. However, this hypothesis did not account for the actual difference in bulk compositions between phase assemblages A and B: assemblage B contains 1.35 weight percent H_2O. Addition of H_2O to the magma has the general effect of supressing crystal-lization. Our calculations illustrate this effect. Al-though assimilation of the hydrous assemblage B results in a larger temperature drop, per gram as-similated, it produces a smaller mass of crystals than assimilation of the anhydrous assemblage A.

This observation is not a general one. If the initial magma composition prior to assimilation includes a few weight percent H_2O, solution of a small amount of H_2O in the assimilate does not affect the course of reaction very much. Under these circum-

ISENTHALPIC ASSIMILATION OF
PELITIC ASSEMBLAGE A (1250 °C)

ASSIMILATION OF PELITIC ASSEMBLAGE A (1250°C)

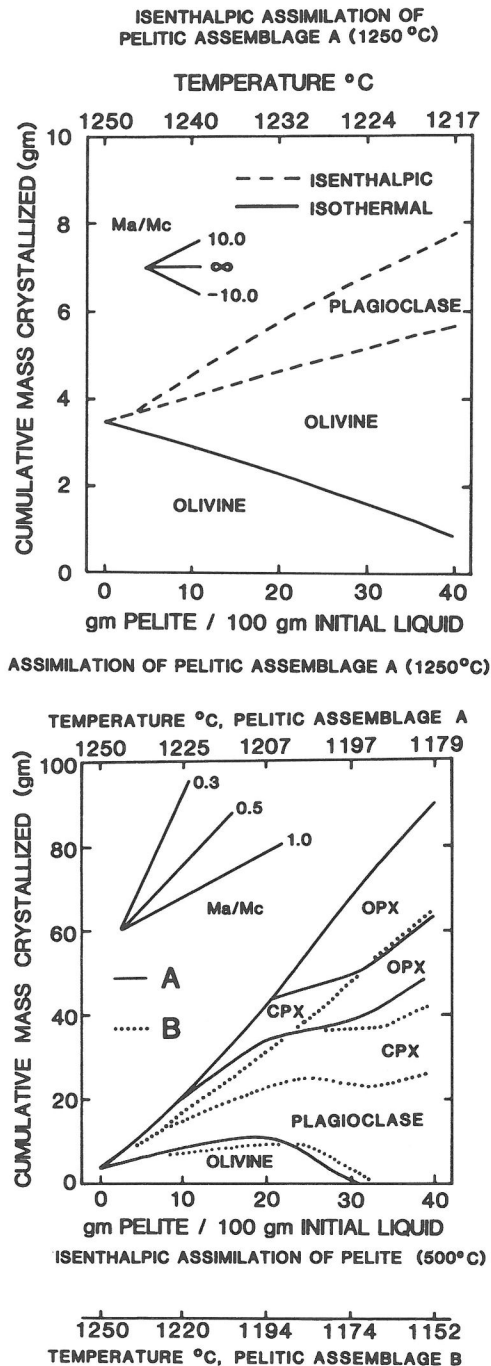
ISENTHALPIC ASSIMILATION OF PELITE (500°C)

FIG. 6. Calculated total solid composition for isothermal and isenthalpic assimilation of pelitic rock in a magnesian MORB (FAMOUS 527-1-1), dry, at 3 kbar, on the FMQ oxygen buffer. Composition and phase assemblages of the pelitic assimilate are given in Table 3. Phase assemblages A and B have identical bulk composition (except that B includes 1.35 weight percent H_2O), but A is composed of Qtz–Ilm–Kspar–Opx–Spinel–Plag, whereas B is composed of Qtz–Ilm–Musc–Bio–Garnet–Plag. Figure 6(A). Initial
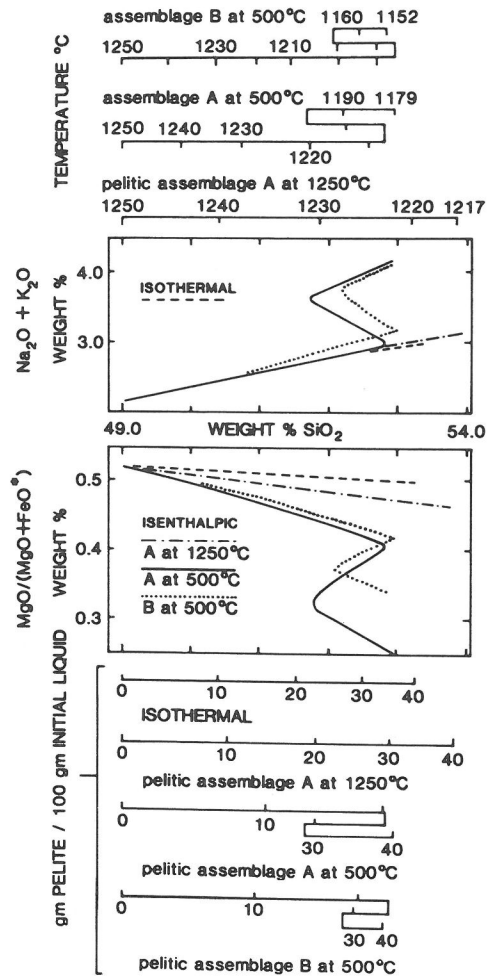

FIG. 7. Calculated liquid composition for isothermal and isenthalpic assimilation of pelitic rock in a magnesian MORB. Input parameters as for Figure 6(A) and (B).

stances, assimilation of a hydrous assemblage will result in a lower final temperature and a larger mass of crystals than assimilation of the same mass of an equivalent anhydrous assemblage.

The different reaction paths for assimilation of pelitic rock result in markedly different liquid compositions, as illustrated in Figure 7 and Table 6. Liquids produced by isenthalpic assimilation of

temperature of the liquid, and the temperature of the assimilate throughout the calculation, was set at 1250°C. *Ma/Mc* refers to the ratio of mass assimilated vs. mass crystallized. Figure 6(B). Input parameters as in 6(A), but with the temperature of the assimilate set at 500°C throughout the calculation.

M. S. Ghiorso and P. B. Kelemen

Table 4. Calculated total solid composition produced during the assimilation of albite in FAMOUS 527-1-1, at 3 kbar, on the FMQ oxygen buffer.

	Initial	Isothermal	Isenthalpic	
Mass Assimilated/100 gm initial liquid + crystals	0	40	40	40
Initial Temperature of Albite	—	1250°C	1250°C	500°C
Total Mass Crystallized (gm)	3.44	7.63	0	99.34
Mass Olivine (gm) Mol Fraction Fo	3.44 0.87	2.09 0.82	0	7.65 0.74
Mass Plagioclase (gm) Mol Fraction An	0	5.54 0.59	0	67.02 0.45

Mass Clinopyroxene (gm)
  Mol Fraction Di
  Mol Fraction Fs
	0	0	0	13.16
				0.83
				0.16

Mass Orthopyroxene (gm)	0	0	0	11.51 0.76
Temperature of the System	250°C	1250°C	1212°C	1170°C

pelitic rock at an initial temperature of 500°C diverge from those produced by assimilation of the same composition at 1250°C early in their fractionation history, becoming strongly iron–enriched and alkaline. Whereas the other two cases show continuously increasing silica contents in derivative liquids, the assimilation of "cold" pelitic rock undergoes a decrease in silica content beginning with the appearance of orthopyroxene on the liquidus, as a result of the reaction olivine + $SiO_{2(liq)}$ = orthopyroxene. Note that this reaction, which is discontinuous in the Mg_2SiO_4–SiO_2 system, is a continuous reaction occurring over a finite temperature interval in iron–bearing systems. An increase in SiO_2 concentration in the liquid resumes with the disappearance of olivine from the system.

These calculations have been done in equilibrium mode; that is, the total solid composition is in equilibrium with the liquid at every step. If the calculations were performed in fractional crystallization mode, the discontinuous reaction would be limited to a single step (in this case, defined by the addition

Table 5. Calculated total solid composition produced during assimilation of pelite in FAMOUS 527-1-1, at 3 kbar, on the FMQ oxygen buffer. Compositions of pelitic assimilates are given in Table 3.

	Initial	Isothermal	Isenthalpic assemblage		
			A	A	B
Mass Assimilated/100 gm initial liquid + crystals	0	40	40	40	40
Initial Temperature of Pelite	—	1250°C	1250°C	500°C	500°C
Total Mass Crystallized (gm)	3.44	0.83	8.23	90.66	62.99
Mass Olivine (gm) Mol Fraction Fo	3.44 0.87	0.83 0.85	6.08 0.82	0	0
Mass Plagioclase (gm) Mol Fraction An	0	0	2.15 0.72	49.11 0.64	26.37 0.68

Mass Clinopyroxene (gm)
  Mol Fraction Di
  Mol Fraction Fs
	0	0	0	14.58
				0.83
				0.16
					15.58
					0.84
					0.14

Mass Orthopyroxene (gm) Mol Fraction En	0	0	0	26.97 0.76	21.04 0.79
Temperature of the System	1250°C	1250°C	1215°C	1181°C	1152°C

Table 6. Calculations of crystal fractionation, assimilation of pelitic rock at 500°C, and assimilation of albite at 500°C, in FAMOUS 527-1-1, at 3 kbar, on the FMQ oxygen buffer. Composition and phase assemblages for pelitic assimilate are given in Table 3.

	Crystal fractionation		Isenthalpic assimilation (assimilate at 500°C)					
			1250 to 1190°C			After 40 gm assimilated		
	Equili-brium	Frac-tion-ation	Pelitic		Albite	Pelitic		Albite
			A	B		A	B	
Weight percent SiO_2	48.0	48.8	52.1	52.7	53.8	53.0	52.9	53.6
Weight percent MgO/(MgO + FeO*) FeO* = total Fe as FeO	0.30	0.32	0.31	0.43	0.43	0.25	0.34	0.39
$Na_2O + K_2O$ weight percent	2.41	2.79	3.89	3.10	4.96	4.18	4.06	6.33
Gm Assimilated	0	0	34	22	28	40	40	40
Gm Crystallized	77	64	78	34	67	91	63	99
Temp °C	1190	1190	1190	1190	1190	1179	1152	1170
Gm Assimilated/°C	0	0	0.57	0.57	0.47	0.56	0.41	0.50
Mass Liquid/Initial Mass Liquid	0.21	0.35	0.55	0.87	0.60	0.48	0.76	0.40

of 2 grams of pelitic rock), and the calculated silica content of the liquid would not decrease over a long interval of assimilation. However, derivative liquids would still be far more iron–enriched and alkaline than those produced by reaction with a wall rock already at magmatic temperature.

Table 6 allows further comparison of the liquid compositions produced by assimilation of wall rock at 500°C. This comparison makes it abundantly clear that calculation of the effect of assimilation on derivative liquids demands accurate character-ization of the bulk composition and the phase as-semblage of the assimilate, as well as the tempera-ture of both wall rock and magma. It is also instruc-tive to compare the calculated liquid and solid lines of descent for isenthalpic assimilation with those calculated for equilibrium or fractional crystalli-zation alone. Whereas some of the liquids produced by assimilation have almost the same Mg# as the liquids produced by crystal fractionation alone, all the liquids derived by assimilation are relatively rich in silica and alkalies.

Neither the equilibrium nor fractional crystalli-zatin of FAMOUS 527-1-1 were calculated to pro-duce orthopyroxene at 1190°C. The total solid composition resulting from equilibrium crystalli-zation at this temperature is 22 weight percent ol-ivine (Fo_{75}), 23 weight percent clinopyroxene (Di_{83}), and 55 weight percent plagioclase (An_{69}). The as-similation of pelitic assemblage A leads to a pre-dicted solid composition with 29 weight percent or-thopyroxene (En_{78}), 16 weight percent clinopyrox-ene (Di_{83}), and 55 weight percent plagioclase (An_{65}) at 1190°C. Similar phase proportions were calcu-lated for assimilation of pelitic assemblage B. This is in partial accord with BOWEN's prediction (1922a,

pp. 549–558) that the assimilation of aluminous sediment in basaltic magma would increase the modal proportion of orthopyroxene and plagioclase, and decrease the proportion of clinopyroxene, pro-duced during crystallization.

CONCLUSIONS

Assimilation of wall rock in fractionating magma may fundamentally alter the solid and liquid line of descent, producing various distinctive magma series, all derived from a common parental liquid. Thermodynamic modelling of such processes is es-sential in predicting solid–liquid reaction stoichi-ometry, and thus the compositional effects of such reactions on derivative liquids and solids. Constant temperature assimilation of refractory solids in liq-uids saturated in less refractory members of the same "reaction series" will often be exothermic. Assimilation of less refractory phases in the same reaction series, and assimilation of phases across a cotectic "valley", will always be endothermic at constant temperature. Particularly for endothermic reactions, modelling of isenthalpic, rather than iso-thermal, conditions may yield results more generally applicable to natural phenomena. Also useful, though not explicitly presented here, are calcula-tions based on externally controlled conditions of decreasing temperature.

The sample calculations presented here reem-phasize the point made by BOWEN (1922a) that the most important variable in the energy balance of reaction between magma and wall rock, besides bulk composition, is the temperature difference between the two. Assimilation of solids with the same com-position, but different initial temperatures, is cal-

culated to produce distinctly different products. In addition, assimilation of solids with the same initial temperature and very similar bulk composition, but different phase assemblages, can also produce a variety of derivative liquids. BOWEN (1922a) argued that the theoretical eutectic "destination" of liquids modified by assimilation reactions remains unchanged. This postulate may well be correct. However, the variety of different lines of descent produced during our calculations suggests new ways of explaining the paths taken by individual magma series.

The ability to model isenthalpic crystallization in magmatic systems may also prove useful in the numerical simulation of the cooling history of magma bodies. In the past, substantial difficulty has been encountered in modelling the thermal history of "real" magmatic systems due, in part, to the necessity of knowing the temporal and spatial dependence of the enthalpy of fusion of the magma in order to calculate the evolving temperature field. These enthalpies of fusion are dependent upon the extent of crystallization and consequently, the temperature of the magma. Thus magma chamber cooling models must be solved iteratively if they involve realistic parameterizations of the enthalpies of fusion of the solid phases. With the ability to determine heterogeneous equilibrium under isenthalpic constraints, an alternative method of calculation exists. If temperature and phase proportions can be calculated given a fixed enthalpy content of the magma at any given time or point in space, then knowledge of the heat flux and the geometry of the chamber will allow simultaneous determination of the phase proportions, phase compositions and temperature field in the cooling magma body. Such calculations need not be performed recursively and are amenable to inclusion in more traditional fluid dynamical models of magma dynamics.

REFERENCES

ANDERSON O. (1915) The system anorthite–forsterite–silica. *Amer. J. Sci., Ser. IV* **39**, 407–454.

BENDER J. F., HODGES F. N. and BENCE A. E. (1978) Petrogenesis of basalts from the project FAMOUS area: Experimental study from 0 to 15 kbars. *Earth Planet. Sci. Lett.* **41**, 277–302.

BOWEN N. L. (1922a) The behavior of inclusions in igneous magmas. *J. Geol.* **30**, 513–570.

BOWEN N. L. (1922b) The reaction principle in petrogenesis. *J. Geol.* **30**, 177–198.

CALLEN H. B. (1961) *Thermodynamics.* 376 pp. John Wiley and Sons.

CARMICHAEL I. S. E and GHIORSO M. S. (1986) Oxidation–reduction relations in basic magma: a case for homogeneous equilibria. *Earth Planet. Sci. Lett.* **78**, 200–210.

CLARKE F. W. (1924) Data of geochemistry: Fifth edition. *U.S. Geol. Surv. Bull. 770*, 841 pp.

GHIORSO M. S. (1985) Chemical mass transfer in magmatic processes I. Thermodynamic relations and numerical algorithms. *Contrib. Mineral. Petrol.* **90**, 107–120.

GHIORSO M. S. and CARMICHAEL I. S. E. (1980) A regular solution model for mea-aluminous silicate liquids: Applications to geothermometry, immiscibility, and the source regions of basic magmas. *Contrib. Mineral. Petrol.* **71**, 323–342.

GHIORSO M. S. and CARMICHAEL I. S. E. (1985) Chemical mass transfer in magmatic processes II. Applications in equilibrium crystallization, fractionation and assimilation. *Contrib. Mineral. Petrol.* **90**, 121–141.

GHIORSO M. S., CARMICHAEL I. S. E., RIVERS M. L. and SACK R. O. (1983) The Gibbs Free Energy of natural silicate liquids; an expanded regular solution approximation for the calculation of magmatic intensive variables. *Contrib. Mineral. Petrol.* **84**, 107–145.

GILL P. E., MURRAY W. and WRIGHT M. H. (1981) *Practical Optimization.* 401 pp. Academic Press Inc.

HELGESON H. C., DELANY J. M., NESBITT H. W. and BIRD D. K. (1978) Summary and critique of the thermodynamic properties of rock–forming minerals. *Amer. J. Sci.* **278-A**, 1–229.

KELEMEN P. B. (1986) Assimilation of ultramafic rock in subduction–related magmatic arcs. *J. Geol.,* (In press).

KELEMEN P. B. and GHIORSO M. S. (1986) Assimilation of peridotite in zoned calc-alkaline plutonic complexes: evidence from the Big Jim Complex, Washington Cascades. *Contrib. Mineral. Petrol.* **94**, 12–28.

KILINC A., CARMICHAEL I. S. E., RIVERS M. L. and SACK R. O. (1983) The ferric–ferrous ratio of natural silicate liquids equilibrated in air. *Contrib. Mineral. Petrol.* **83**, 136–140.

KORZHINSKII D. S. (1959) *Physiochemical Basis of the Analysis of the Paragenesis of Minerals.* 142 pp. Consultants Bureau.

OSBORN E. F. and TAIT D. B. (1952) The system diopside–forsterite–anorthite. *Amer. J. Sci.,* **250-A**, 413–433.

ROBIE R. A., HEMINGWAY B. S. and FISHER J. R. (1978) Thermodynamic properties of minerals and related substances at 298.15 K and 1 bar (10^5 Pascals) pressure and at high temperature. *U.S. Geol. Surv. Bull. 1452.* 456 pp.

STEBBINS J. F., CARMICHAEL I. S. E. and MORET L. K. (1984) Heat capacities and entropies of silicate liquids and glasses. *Contrib. Mineral. Petrol.* **86**, 131–148.

THOMPSON J. B. JR. (1970) Geochemical reaction and open systems. *Geochim. Cosmochim. Acta* **34**, 529–551.

APPENDIX A NUMERICAL METHODS
FOR MINIMIZING Φ

We seek solutions (optimal values of n and possibly temperature (T) and pressure (P)) to the following problem in non–linear optimization:

$$\text{minimize} \quad \Phi(x, y, n)$$

such that

$$Cn - b = 0$$

$$\Delta x(n, T, P) = 0$$

and

$$\Delta y(n, T, P) = 0. \tag{A1}$$

We will let the vector z denote all the variables being optimized in the minimization of Φ. z may contain the elements of n as well as T and P. The last two equality constraints ($\Delta x = 0$, $\Delta y = 0$) are non–linear, so the usual minimization method of projecting with the constraint matrix and solving the unconstrained quadratic sub–problem (GHIORSO, 1985) fails. Instead, the suggestion of GILL et al. (1981) will be followed and the unconstrained related Lagrange function corresponding to Equation (A1) will be optimized. We denote the Lagrangian of Φ by Ξ and define it such that

$$\Xi(x, y, n, \lambda_n, \lambda_x, \lambda_y) = \Phi - \lambda_n^T(Cn - b) - \lambda_x \Delta x - \lambda_y \Delta y. \tag{A2}$$

The new variables λ_n, λ_x, and λ_y are generally referred to as Lagrange multipliers. The minimum of Ξ is obtained iteratively by seeking steps, s, away from an initial non–optimal, but feasible guess to the solution vector of Equation (A1), which we will denote z_o, and stepping along this direction while continuously maintaining the feasibility of the solution parameters. In this problem, feasible parameters refer to the set of solutions that satisfy the constraints. To define the search direction s we construct a vector c such that

$$c = \begin{bmatrix} Cn - b \\ \Delta x(n, T, P) \\ \Delta y(n, T, P) \end{bmatrix}$$

and define a matrix, A, which represents the derivative of this vector of equality constraints with respect to the optimal variables. A is commonly referred to as the Jacobian of the system of non–linear constraints and should be evaluated at the initial feasible point, z_o. Thus,

$$A = \left(\frac{dc}{dz}\right)^T \Bigg|_{z_o} = \begin{bmatrix} C^T \\ \left(\dfrac{\partial x}{\partial z}\right)^T \Big|_{z_o} \\ \left(\dfrac{\partial y}{\partial z}\right)^T \Big|_{z_o} \end{bmatrix} .$$

A matrix, Z, can be computed from the orthogonal decomposition of A (GILL et al., 1981), which projects the optimal parameters of Φ into the null–space of the quality constraints. Unlike linearly constrained optimization, this null–space projection operator is only reliable "close" to the initial feasible guess z_o. An approximation, Zp, to the feasible search direction, s, is computed by solving the quadratic (second order) Newton approximation to the minimum of the Lagrangian:

$$Z^T W Z p = -Z^T g. \tag{A3}$$

The vector, g, is defined as the gradient of the original potential function [Equation (A1)] with respect to the optimal variables, z, evaluated at the initial feasible point, and the matrix W is defined as the second derivative matrix of the Lagrangian [Equation (A2)] with respect to the optimal variables and evaluated at the initial feasible point. This matrix is often referred to as the Hessian matrix of the Lagrangian function, Ξ. The Lagrange multipliers which are needed to compute the matrix, W, are estimated by solving the system of linear equations:

$$g = A^T \begin{bmatrix} \lambda_n \\ \lambda_x \\ \lambda_y \end{bmatrix} .$$

The descent direction, Zp, obtained from Equation (A3), may not be feasible because of the non–linearity of the quality constraints. Thus the new feasible guess to the solution of Equation (A1), which we will denote $z_o + s$, is found by determining the value of the steplength parameter, γ, which minimizes the potential, Φ, along the search direction, s, subject to maintaining the feasibility of the non–linear constraints; the linear constraints are implicitly maintained by the null–space operator, Z. This feasibility is guaranteed by solving, for every proposed value of γ, the system of non–linear equations

$$\Delta x(z_o + \gamma Z p + Y p_\gamma) = 0,$$

and

$$\Delta y(z_{\rm o} + \gamma Z p + Y p_{\gamma}) = 0, \tag{A4}$$

for the elements of the vector, p_{γ}. The search direction, s, is defined as $\gamma Z p + Y p_{\gamma}$, where Y is a matrix which spans the range–space of A and p_{γ} is a vector whose length is equal to the total number of equality constraints. Y may be taken to be A^T (GILL *et al.*, 1981) which emphasizes that the range–space describes the space of feasible solutions to Equation (A1). The p_{γ} obtained from the solution of Equation (A4) have no particular physical significance except insofar as their non–zero values indicate the sensitivity of the system of equality constraints to the optimal solution parameters about the initial feasible point.

The minimum of the potential function, Φ, is determined by solving successive quadratic approximations to the Lagrangian [Equations (A3) and (A4)] until the computed norm of the feasible step direction, s, is smaller than machine precision. This minimum is verified by examining the sufficient conditions to insure convergence. These are (1) The equality constraints are satisfied; (2) The norm of the projected gradient is approximately zero ($Z^T g \simeq 0$); and (3) The projected Hessian of the Lagrangian function ($Z_T W Z$) is positive definite.

For the convenience of the reader appropriate expressions are provided below for the quantities, g and W, in the three explicit cases of the potential, Φ, discussed in the text.

The isenthalpic case ($\Phi = -S$)

In this case the optimal variables are the system components, n and the temperature, T. The first derivative of Φ is given by the partitioned vector:

$$g = \begin{bmatrix} -\left(\dfrac{\partial S}{\partial n}\right)_{T,P} \\[2ex] \hline -\dfrac{C_P}{T} \end{bmatrix} \tag{A5}$$

evaluated at $n_{\rm o}$ and $T_{\rm o}$. The Jacobian of the system of equality constraints may be written:

$$A = \begin{bmatrix} C^T & | & 0 \\ \hline \left(\dfrac{\partial H}{\partial n}\right)^T_{T,P} & | & C_P \end{bmatrix}. \tag{A6}$$

The elements of this matrix should be evaluated at $n_{\rm o}$ and and $T_{\rm o}$. The second derivative of the associated Lagrangian is provided by the partitioned symmetrix matrix:

$$W = \begin{bmatrix} \left(\dfrac{\partial^2 S}{\partial n^2}\right)_{T,P} - \lambda \left(\dfrac{\partial^2 H}{\partial n^2}\right)_{T,P} & \Big| & -\left(\dfrac{1}{T} + \lambda\right)\left(\dfrac{\partial C_P}{\partial n}\right)_{T,P} \\ \hline & & -\left(\dfrac{1}{T} + \lambda\right)\left(\dfrac{\partial C_P}{\partial T}\right)_{n,P} + \dfrac{C_P}{T^2} \end{bmatrix}. \tag{A7}$$

The elements of this matrix should be evaluated at $n_{\rm o}$ and $T_{\rm o}$.

The isochoric case ($\Phi = A$)

For the case of constant volume, the optimal variables are the system components, n and the pressure, P. The gradient of Φ is given by the partitioned vector:

$$g = \begin{bmatrix} \left(\dfrac{\partial G}{\partial n}\right)_{T,P} - P\left(\dfrac{\partial V}{\partial n}\right)_{T,P} \\[2ex] \hline -P\left(\dfrac{\partial V}{\partial P}\right)_{T,n} \end{bmatrix} \tag{A8}$$

evaluated at $n_{\rm o}$ and $P_{\rm o}$. The derivative matrix of the equality constraints is provided by:

$$A = \begin{bmatrix} C^T & | & 0 \\ \hline \left(\dfrac{\partial V}{\partial n}\right)^T_{T,P} & | & \left(\dfrac{\partial V}{\partial P}\right)_{T,n} \end{bmatrix}. \tag{A9}$$

This matrix should be evaluated at $n_{\rm o}$ and $P_{\rm o}$. The Hessian matrix of the Lagrangian is given by the symmetric partitioned matrix:

$$W = \begin{bmatrix} \left(\dfrac{\partial^2 G}{\partial n^2}\right)_{T,P} - (P+\lambda)\left(\dfrac{\partial^2 V}{\partial n^2}\right)_{T,P} & -(P+\lambda)\left(\dfrac{\partial^2 V}{\partial P \partial n}\right)_{T,P} \\ \hline & -\left(\dfrac{\partial V}{\partial P}\right)_{n,T} - (P+\lambda)\left(\dfrac{\partial^2 V}{\partial P^2}\right)_{n,T} \end{bmatrix}. \tag{A10}$$

This matrix should be evaluated at n_o and P_o.

The isenthalpic and isochoric case ($\Phi = -S - PV/T$)

In this most complicated example, the optimal variables are the system components, n, the temperature, T and the pressure, P. The gradient of Φ is given by the partitioned vector:

$$g = \begin{bmatrix} -\left(\dfrac{\partial S}{\partial n}\right)_{T,P} - P\left(\dfrac{\partial V}{\partial n}\right)_{T,P} \\ \hline -\dfrac{C_P}{T} + \dfrac{VP}{T^2} - \dfrac{P}{T}\left(\dfrac{\partial V}{\partial T}\right)_{n,P} \\ \hline \left(\dfrac{\partial V}{\partial T}\right)_{n,P} - \dfrac{V}{T} - \dfrac{P}{T}\left(\dfrac{\partial V}{\partial P}\right)_{T,n} \end{bmatrix} \tag{A11}$$

evaluated at the initial point n_o, T_o and P_o. The derivative matrix of equality constraints is provided by:

$$A = \begin{bmatrix} C^T & | & 0 & 0 \\ \hline \left(\dfrac{\partial H}{\partial n}\right)^T_{T,P} & | & C_P & V - T\left(\dfrac{\partial V}{\partial T}\right)_{P,n} \\ \hline \left(\dfrac{\partial V}{\partial n}\right)^T_{T,P} & | & \left(\dfrac{\partial V}{\partial T}\right)_{P,n} & \left(\dfrac{\partial V}{\partial P}\right)_{T,n} \end{bmatrix}. \tag{A12}$$

This matrix should be evaluated at n_o, T_o and P_o. The symmetric second derivative matrix of the Lagrangian is given by:

$$W = \begin{bmatrix} W_{n,n} | W_{n,T} | W_{n,P} \\ \hline W_{T,T} | W_{T,P} \\ \hline W_{P,P} \end{bmatrix} \tag{A13}$$

where

$$W_{n,n} = \left(\frac{\partial^2 S}{\partial n^2}\right)_{T,P} - \lambda_T\left(\frac{\partial^2 H}{\partial n^2}\right)_{T,P} - \left(\frac{P}{T} + \lambda_P\right)\left(\frac{\partial^2 V}{\partial n^2}\right)_{T,P} \tag{A14}$$

$$W_{n,T} = -\left(\frac{1}{T} + \lambda_T\right)\left(\frac{\partial C_p}{\partial n}\right)_{T,P} + \frac{P}{T^2}\left(\frac{\partial V}{\partial n}\right)_{T,P} - \left(\frac{P}{T} + \lambda_P\right)\left(\frac{\partial^2 V}{\partial n \partial T}\right)_P \tag{A15}$$

$$W_{n,P} = -\frac{1}{T}\left(\frac{\partial V}{\partial n}\right)_{T,P} + (1 + \lambda_T T)\left(\frac{\partial^2 V}{\partial n \partial T}\right)_P - \left(\frac{P}{T} + \lambda_P\right)\left(\frac{\partial^2 V}{\partial n \partial P}\right)_T \tag{A16}$$

$$W_{T,T} = \frac{C_p}{T^2} - \frac{2VP}{T^3} + \frac{2P}{T^2}\left(\frac{\partial V}{\partial T}\right)_{n,P} - \left(\frac{1}{T} + \lambda_T\right)\left(\frac{\partial C_p}{\partial T}\right)_{n,P} - \left(\frac{P}{T} + \lambda_P\right)\left(\frac{\partial^2 V}{\partial T^2}\right)_{n,P} \tag{A17}$$

$$W_{T,P} = (1 + \lambda_T T)\left(\frac{\partial^2 V}{\partial T^2}\right)_{n,P} - \frac{V}{T^2} + \left(\lambda_T - \frac{1}{T}\right)\left(\frac{\partial V}{\partial T}\right)_{n,P} + \frac{P}{T^2}\left(\frac{\partial V}{\partial P}\right)_{n,T} - \left(\frac{P}{T} + \lambda_P\right)\left(\frac{\partial^2 V}{\partial T \partial P}\right)_n \tag{A18}$$

and

$$W_{P,P} = (1 + \lambda_T T)\left(\frac{\partial^2 V}{\partial T \partial P}\right)_n - \frac{2}{T}\left(\frac{\partial V}{\partial P}\right)_{n,T} - \left(\frac{P}{T} + \lambda_P\right)\left(\frac{\partial^2 V}{\partial P^2}\right)_{n,T}. \tag{A19}$$

Equations (A14)–(A19) should be evaluated at the point n_o, T_o and P_o.

APPENDIX B HETEROGENEOUS EQUILIBRIUM IN OPEN SYSTEMS SUBJECT TO GENERALIZED THERMODYNAMIC CONSTRAINTS

The gradient necessary for the minimization of the potential Φ given by Equation (11) is:

$$g = \left(\frac{\partial G}{\partial n}\right)_{T,P} - \left(\frac{\partial n_{O_2}}{\partial n}\right)_{T,P}\mu_{O_2} - n_{O_2}\left(\frac{\partial \mu_{O_2}}{\partial n}\right)_{T,P}. \quad (B1)$$

The derivative of the constraint matrix is provided by:

$$A = \begin{bmatrix} C^{*T} \\ \left(\frac{\partial \mu_{O_2}}{\partial n}\right)_{T,P}^T \end{bmatrix} \quad (B2)$$

where C^* represents a linear bulk composition constraint matrix modified for constancy of total iron and variable ferric/ferrous ratio. The Hessian matrix of Equation (11) may be written:

$$W = \left(\frac{\partial^2 G}{\partial n^2}\right)_{T,P} - 2\left(\frac{\partial n_{O_2}}{\partial n}\right)_{T,P}\left(\frac{\partial \mu_{O_2}}{\partial n}\right)_{T,P}$$
$$- (n_{O_2} + \lambda_{O_2})\left(\frac{\partial^2 \mu_{O_2}}{\partial n^2}\right)_{T,P}. \quad (B3)$$

Equations (B1) through (B3) should be evaluated at the initial feasible point, n_o.

The potentials defined by Equations (6), (7) and (8) can be transformed to allow for the modelling of isenthalpic and isochoric processes in magmatic systems open to oxygen. We will illustrate the most complicated case. The "isenthalpic/isochoric" potential defined by Equation (8) can be modified for open systems by recognizing that:

$$\left(\frac{\partial G/T}{\partial n_{O_2}/T}\right)_{(1/T),P,n^*} = \mu_{O_2}$$

from which a new open system potential, Φ, can be defined as:

$$\Phi(H, V, n) = \frac{G}{T} - \frac{1}{T}\left(\frac{\partial G/T}{\partial 1/T}\right)_{P,n} - P\left(\frac{\partial G/T}{\partial P}\right)_{(1/T),n}$$
$$- \frac{n_{O_2}}{T}\left(\frac{\partial G/T}{\partial n_{O_2}/T}\right)_{(1/T),P,n^*}$$
$$= \frac{G}{T} - \frac{1}{T}H - P\frac{V}{T} - \frac{n_{O_2}}{T}\mu_{O_2}$$

$$\Phi(H, V, n) = -S - \frac{VP}{T} - \frac{n_{O_2}\mu_{O_2}}{T}. \quad (B4)$$

The optimal variables of this new potential Φ are n, T and P; the oxygen chemical potential constraint does not introduce new optimal variables and only modifies the relationships among the elements of n. If g and W denote the gradient and Hessian defined by Equations (A11) and (A13), then the gradient of Equation (B4) is defined by:

$$g_{(B4)} = g + \begin{bmatrix} g_{O_2} \\ g_T \\ g_P \end{bmatrix}, \quad (B5)$$

where, given that $G_{O_2} = n_{O_2}\mu_{O_2}$, we have;

$$g_{O_2} = -\frac{1}{T}\left(\frac{\partial G_{O_2}}{\partial n}\right)_{T,P}, \quad (B6)$$

$$g_T = \frac{G_{O_2}}{T^2} + \frac{S_{O_2}}{T}, \quad (B7)$$

$$g_P = -\frac{V_{O_2}}{T}. \quad (B8)$$

This gradient must be evaluated at the initial feasible point n_o, T_o, P_o. The Hessian matrix corresponding to the associated Lagrangian of Φ is given by:

$$W_{(B4)} = W + \begin{bmatrix} W_{n,n,O_2} & | W_{n,T,O_2} | & W_{n,P,O_2} \\ & \overline{W_{T,T,O_2}\, W_{T,P,O_2}} \\ & & W_{P,P,O_2} \end{bmatrix}, \quad (B9)$$

where,

$$W_{n,n,O_2} = -\left(\frac{\partial^2 G_{O_2}}{\partial n^2}\right)_{T,P} - \lambda_{O_2}\left(\frac{\partial^2 \mu_{O_2}}{\partial n^2}\right)_{T,P}, \quad (B10)$$

$$W_{n,T,O_2} = \frac{1}{T^2}\left(\frac{\partial G_{O_2}}{\partial n}\right)_{T,P} + \frac{1}{T}\left(\frac{\partial S_{O_2}}{\partial n}\right)_{T,P} + \lambda_{O_2}\left(\frac{\partial \bar{s}_{O_2}}{\partial n}\right)_{T,P}, \quad (B11)$$

$$W_{n,P,O_2} = -\frac{1}{T}\left(\frac{\partial V_{O_2}}{\partial n}\right)_{T,P} - \lambda_{O_2}\left(\frac{\partial \bar{v}_{O_2}}{\partial n}\right)_{T,P}, \quad (B12)$$

$$W_{T,T,O_2} = -\frac{2}{T^3}G_{O_2} - \frac{2}{T^2}S_{O_2} + \frac{1}{T^2}C_{P,O_2} + \lambda_{O_2}\frac{1}{T}\bar{C}_{P,O_2}, \quad (B13)$$

$$W_{T,P,O_2} = \frac{V_{O_2}}{T^2} - \frac{1}{T}\left(\frac{\partial V_{O_2}}{\partial T}\right)_{n,P} - \lambda_{O_2}\left(\frac{\partial \bar{v}_{O_2}}{\partial T}\right)_{n,P}, \quad (B14)$$

and,

$$W_{P,P,O_2} = -\frac{1}{T}\left(\frac{\partial V_{O_2}}{\partial P}\right)_{T,n} - \lambda_{O_2}\left(\frac{\partial \bar{v}_{O_2}}{\partial P}\right)_{T,n}. \quad (B15)$$

For use in the algorithm described in Appendix A the matrix defined in Equation (B9) must be evaluated at the initial feasible point.